# Gas Separation Properties of Ionic Liquids and Porous Liquids

**A Thesis Presented for the**

**Master of Science**

**Degree**

**The University of Tennessee, Knoxville**

**Kristina Armstrong**

**August 2025**

## ACKNOWLEDGMENTS

I would like to express my gratitude to my advisor, Dr. Sheng Dai, for his guidance and expertise throughout my master's research. His constant support and patience was fundamental in shaping my academic growth. I would also like to thank Dr. Shannon Mahurin and Dr. Arvind Ganesan for the knowledge and assistance they shared with me throughout my research. Additionally, I would like to extend my gratitude to the rest of the Dai lab for the encouragement and knowledge they shared along the way. Finally, I would like to thank my friends and family for their constant encouragement and support throughout my career. Without them, my achievements would not have been possible. Thank you to everyone I've encountered along my academic journey.

## ABSTRACT

With a constant rise in carbon emissions, developing effective gas separation techniques for carbon capture is critical for combating climate change. Type III porous liquids represent a promising new class of porous material that combines the free volume of porous solids and the nonvolatile properties of ionic liquids. The resulting permanent porosity can be used to adjust the gas separation properties of an ionic liquid, including the $\frac{CO_2}{N_2}$ selectivity and $CO_2$ and $N_2$ permeabilities. In this project, the zeolites Hydrogen-Zeolite Socony Mobil-5 (H-ZSM-5) and Sodium-Zeolite Socony Mobil-5 (Na-ZSM-5) were suspended in the ionic liquids, Trihexyl-tetradecylphosphonium bromide ($[P_{66614}][Br]$) and 8,8′-(3,6-dioxaoctane-1,8-diyl)bis(1,8-diazabicyclo[5.4.0]undec-7-en-8-ium)bis(trifluoromethanesulfonyl)imide ([DBU-PEG][$NTf_2$]) respectively. The membranes of the ionic liquids and their porous liquids at varying concentrations were tested and analyzed for their $\frac{CO_2}{N_2}$ selectivity and their $CO_2$ and $N_2$ permeabilities. The goal of this work is to understand the gas transport in porous liquids, explore how the addition of zeolites impacts gas separation of an ionic liquid, and assess how varying the concentration of free volume in the porous liquids influences gas separation performance. The results show that incorporating H-ZSM-5 with $[P_{66614}][Br]$ enhances the $\frac{CO_2}{N_2}$ selectivity as well as the $CO_2$ and $N_2$ permeabilities as the zeolite concentration increases. The addition of Na-ZSM-5 in [DBU-PEG][$NTf_2$] improved the $\frac{CO_2}{N_2}$ selectivity but led to a decrease in $CO_2$ and $N_2$ permeabilities. These results demonstrate that the addition of zeolites into ionic liquids can be used to adjust gas separation properties for carbon capture.

## TABLE OF CONTENTS

## LIST OF TABLES

## LIST OF FIGURES

# CHAPTER 1. INTRODUCTION AND BACKGROUND

## *1.1. Introduction.*

Since the start of the industrial revolution around 1750, the concentration of atmospheric carbon dioxide has increased exponentially by about 50%. Between 1979 and 2024, the atmospheric carbon dioxide increased by 20%, accounting for over 50% of the increase since the industrial revolution.[12] The concentration of atmospheric carbon dioxide consistently fluctuated between 180 ppm and 280 ppm over the last 800,000 years. It never reached above 300 ppm before the start of the industrial revolution.[12] This increase is caused from the burning of fossil fuels like coal and oil that release carbon dioxide into the atmosphere. Much of these greenhouse gas emissions come from transportation, electricity, and industries. About 80% of the greenhouse gases released are carbon dioxide.[19]

The carbon cycle is the process that balances the amount of carbon stored underground and in plants versus released into the atmosphere. This balance is what stabilizes Earth's temperature.[16] The concentration of atmospheric carbon is directly related to the Earth's temperature. If all the carbon dioxide was stored, Earth would be frozen with an average temperature of -18°C. And if all the carbon dioxide was in the atmosphere, Earth would have an average temperature of 400°C.[16] The higher-than-average concentration of atmospheric carbon dioxide has already caused the global temperature to increase. Since 1880, the global temperature has increased 1.1°C with most of this change occurring after 1975.[14] The last ice age came about from a 5 degree drop in the global temperature, so this one-degree change is quite significant. It is especially significant when considering the amount of energy it takes to heat the atmosphere, oceans, and land to that degree.[14]

### *1.2. Types of Porous Liquids.*

Porous liquids are a unique class of material combining the permanent porosity of a porous solid with the fluidity of a liquid.[6] They can be broken into three different categories based on how they are made. Type 1 porous liquids are a neat porous liquid host that cannot be penetrated or collapsed. They are a single-phase fluid system with no boundary separating the solid nanomaterial from the dispersing solvent. These porous liquids have an internal cavity, are rigid, and cannot intermolecularly self-fill.[15] While type 1 porous liquids are single phased, type 2 and type 3 porous liquids are made of a solvent and a porous material. Type 2 porous liquids are porous molecular cages dissolved in a sterically hindered solvent.[6] This porous liquid must be rigid, and the solvent cannot occupy the cavities of the molecular cages.[15] Type 3 porous liquids are solid microporous nanomaterials dispersed in a sterically hindered solvent.[15] Specifically in this work, the type 3 porous liquids are composed of metal organic frameworks suspended in ionic liquids. **Figure 1.1** displays the three types of porous liquids and their porosities.

Porous liquids are tunable for many industrial and environmental uses by altering the ionic composition and pore size. Their porosity while maintaining a liquid phase makes them particularly attractive for applications such as energy storage technology, catalytic reactions, carbon capture, and gas separation and storage. Porous liquids combine the separation benefits from both the ionic liquid and the porous media. Specifically, ionic liquids contribute high adsorption capacity, thermodynamic stability, and non-volatile properties. Meanwhile, the porous media increases the surface area for gas particles to be trapped and stored by introducing free volume.

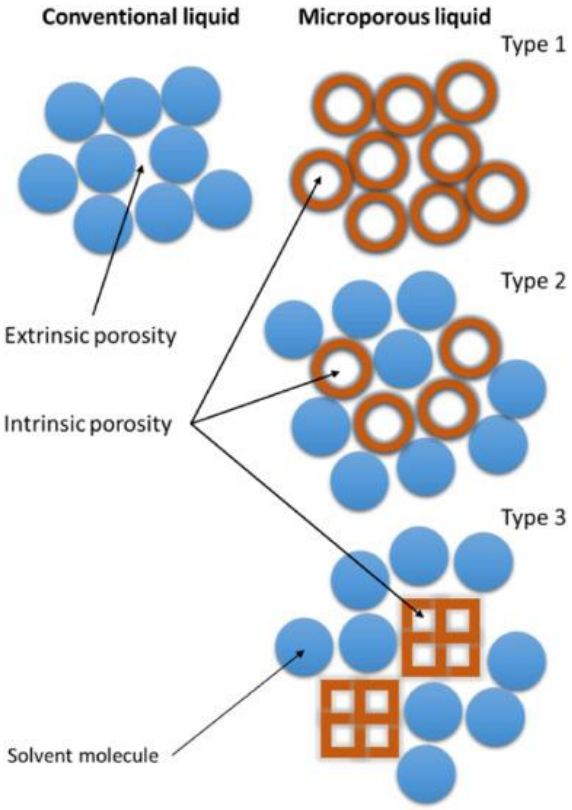


**Figure 1.1. Schematic diagram of the three types of porous liquids.**[1]

### *1.3. Zeolites.*

Zeolites are microporous, crystalline metal organic frameworks (MOFs) that are made of aluminosilicates. MOFs are composed of metal ions and organic linkers that have high porosity. They typically have free volumes of up to 90%. Free volume pores allow gas particles of a particular size to get trapped and stored. Due to the porosity, high stability, and low cost of zeolites, there is an interest in using them for $CO_2$ adsorption and gas separation. The physicochemical properties of zeolites are primarily dependent on the silicon/aluminum ratio. Having a lower Si/Al ratio will increase the amount of aluminum present, increasing the number of cations present.[4] Typically, the active sites for $CO_2$ adsorption are at the cations located in the pores of the framework. Therefore, having more cations results in more adsorption sites and increases the capacity for $CO_2$ adsorption. However, too low of a ratio may result in steric hindrance in these cations.[4] This would cause the $CO_2$ adsorption capacity to decrease, so it is important to find a balance between these factors to maximize the amount of adsorption sites.

In ZSM-5, the framework is composed of 10 membered rings of silicon and aluminum. The porous structure of ZSM-5 is displayed in **Figure 1.2**. The silicon aluminum framework yields a negative charge, and is neutralized with cations, like Na+ and H+. Characteristics of the cations, such as the acidity and size of the radius, affect the strength of $CO_2$ adsorption. Due to the acidity of $CO_2$, a zeolite with stronger basicity has stronger $CO_2$ adsorption properties.[4] Additionally, a cation with a larger radius has lower polarizability and decreases the size of zeolite pores. This causes weaker interactions with the $CO_2$ molecules, more steric hindrance, and decreases the $CO_2$ adsorption capacity.[4] Overall, cations that are weaker acids and have smaller radii contribute to better $CO_2$ adsorption properties.

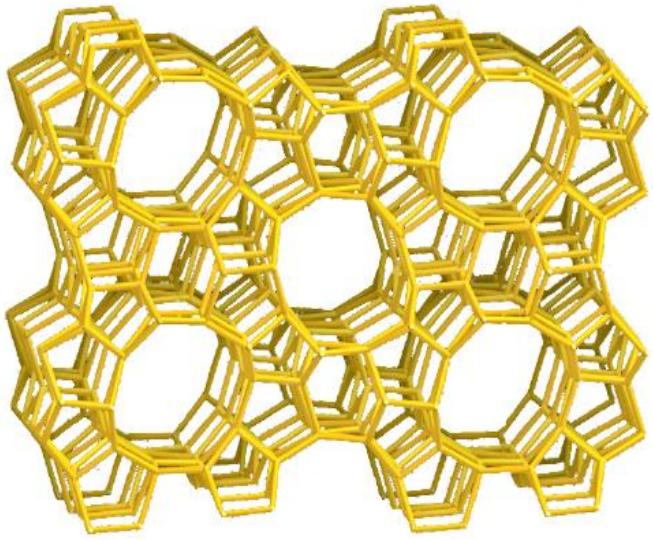

**Figure 1.2. Structure of ZSM-5.[20]**

### *1.4. $CO_2$ Sorption in Ionic Liquids.*

Ionic liquids are comprised of cations and anions appearing as a liquid at room temperature. They are unique due to their thermodynamic stability, non-volatility, and their high $CO_2$ adsorption capacity. Researchers have worked to improve the $CO_2$ uptake by synthesizing functionalized ionic liquids specifically for $CO_2$ capture. These ionic liquids have higher $\frac{CO_2}{N_2}$ selectivity, higher adsorption capacity, quicker adsorption, and more stable cycle of adsorption and desorption.[2] Adsorption of $CO_2$ can be classified as either physisorption or chemisorption. In physisorption, $CO_2$ gas molecules attach to the pore walls of the adsorption site through Van der Waal forces. In chemisorption, $CO_2$ gas molecules form a chemical bond with the adsorption site (**Figure 1.3**).[7] Most ionic liquids adsorb $CO_2$ through physisorption, and their physical characteristics, such as their volatility, gas solubility, and viscosities, affect how well they capture $CO_2$. Ionic liquids typically have no vapor pressure or a very low vapor pressure, helping prevent loss of the capturing solvent through evaporation.[2]

The $CO_2$ solubility of the ionic liquids is dependent on the ions and their Van der Waal forces.[1] For example, the anion $NTf_2$ has a higher solubility than most other ionic liquid anions. The solubility of the cations and anions are directly proportional to Henry's Law. Henry's Law states that the amount of dissolved gas in a liquid is proportional to the partial pressure of that specific gas. In addition to this, each cation has a different amount of free volume. The size of the free volumes is based on the alkyl chains present, and higher free volume usually has higher $CO_2$ solubility.[18] Additionally, ionic liquids are typically more viscous than other liquids like water or alcohols. However, ionic liquids with higher viscosities can restrict $CO_2$ uptake and decrease mass transfer. Higher viscosities will have slower diffusion of $CO_2$ into the ionic liquids. This lowers the rate of mass transfer and lowers the efficiency of $CO_2$ capture.[2]

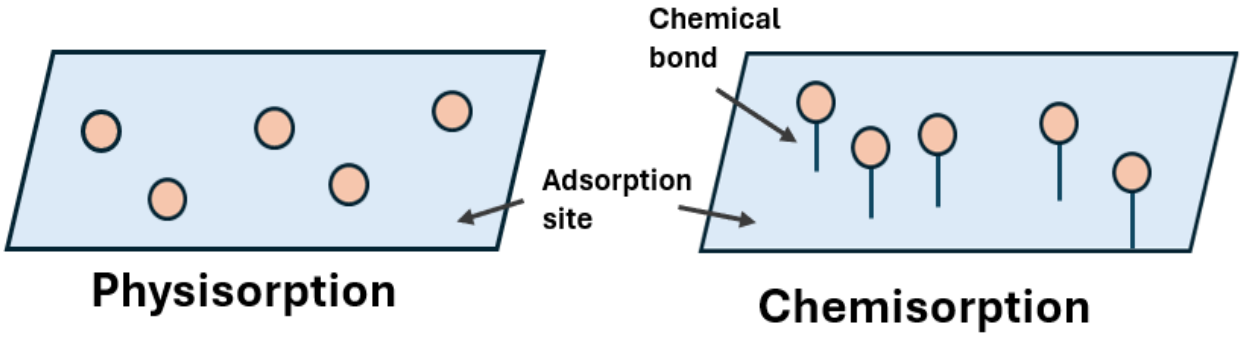


**Figure 1.3. Schematic displaying the difference between physisorption and chemisorption.**

### *1.5. Gas Separation Selectivity.*

Gas separation is essential to isolate carbon dioxide from other emitted gases for it to be captured and stored. Since different gases have varying molecular sizes, using porous liquids presents selectivity for one gas over others through the pore cavity sizes. The gas selectivity and permeability can be measured using polymeric membranes with pressure applied to the gas on one side. The resistance of the gas to flow through the membrane is dependent on the chemical and physical properties of the gas being tested and the membrane composition. This method was used to determine the selectivity and permeability of $CO_2$ and $N_2$.

The permeance of the gasses is calculated using the volume of the permeate (V), the molar gas constant (R), the temperature in kelvin (T), the area of the membrane (A), the initial pressure difference in pascals ($\Delta P$), and the slope of pressure vs time (dP"/dt). The selectivity is calculated by the ratio of the higher gas permeance to the lower gas permeance. In this case, it is the ratio of the $CO_2$ permeance to $N_2$ permeance.

$$\text{Permeance}=\frac{V}{RTA\Delta P}\cdot\frac{dP''}{dt} \qquad \text{Selectivity}=\frac{CO_2\ \text{Permeance}}{N_2\ \text{Permeance}}$$

The permeability of the gases is calculated using the tortuosity ($\tau$), the open area ($\Phi$), the gas permeance, and the membrane thickness.

$$\text{Permeability}=\frac{\tau}{\phi}\cdot\text{Permeance}\cdot\text{Thickness}$$

Both the permeance and permeability describe how the gas flows through the porous liquid in the membrane. Permeance is a measure of the rate at which the gas passes through the membrane. Permeability applies this rate to the thickness of the membrane, so it can be seen as how easily the gas can flow through the membrane. The selectivity describes how much the porous liquid favors one gas over the other. Having a high selectivity for $CO_2$, over another gas, like $N_2$, allows the porous liquid to be specific in what gas it obtains and what it allows to pass

through. This is important in carbon capture methods, as capturing only carbon dioxide aims towards balancing out the carbon cycle. Capturing nitrogen in this process is not needed, as it would start an imbalance in the nitrogen cycle.

### *1.6. Membrane Testing.*

Polyethersulfone (PES) membranes are strong and durable membranes with a uniform pore size. This makes them ideal for testing the gas separation capabilities of the ionic liquids and porous liquids. The ionic liquids are typically loaded onto 100 nm membranes, as they can easily fit into membrane pores of that size. The porous liquids must be loaded onto membranes of a larger pore size, 450 nm. The size of the zeolites is about 200 nm, so they are too big to penetrate the pores of the 100 nm membrane. The porosity factor is dependent on the type and pore size of the membranes, thus accounting for this change in the calculations.

PES membranes are typically cheaper and more manageable than ceramic membranes. Ceramic membranes easily crack and tear when transported or loaded onto the testing systems. This causes issues when testing ceramic membranes, as the smallest crack in the membrane can give poor data. This makes PES membranes better to test gas separation under different pressures. However, ceramic membranes are more chemically and thermally stable than PES membranes, so they are better to use when testing gas separation capabilities under temperatures higher than room temperature.

### *1.7. Thesis Objectives.*

To reduce the amount of carbon dioxide being released into the atmosphere, selective gas separation can isolate carbon dioxide from other gases for carbon capture capabilities. The separation of carbon dioxide from nitrogen gas is a popular example of this. Implementing gas separation and adsorption techniques into industries can prevent the release of carbon dioxide

and reduce the greenhouse effect. The use of ionic liquids is a popular technique for carbon capture due to their low vapor pressure and high stability. In this study, zeolites were added to ionic liquids to create type three porous liquids and improve the gas separation capabilities of ionic liquids. The addition of zeolites introduces free volume pores in the ionic liquids, allowing gas particles to get trapped and stored. These type three porous liquids were tested for their ability to separate carbon dioxide from nitrogen gas and characterized for their permeability of both gases.

The project has three main objectives. The first objective is to understand the gas transport characteristics in ionic liquids and porous liquids. This includes the $CO_2$ and $N_2$ permeabilities and the selectivity of $\frac{CO_2}{N_2}$ gas separation. The second objective is to observe how the addition of zeolites into ionic liquids affects characteristics of the ionic liquids. Characteristics analyzed include $CO_2$ and $N_2$ gas permeabilities, $\frac{CO_2}{N_2}$ gas separation, and viscosities. The third objective is to analyze how the concentration of the free volume in the porous liquids affects the gas separation capabilities. Specifically, how different concentrations of free volume affect the $\frac{CO_2}{N_2}$ selectivity and the $CO_2$ and $N_2$ permeabilities.

# CHAPTER 2. EXPERIMENTAL PROCEDURES

## *2.1. Obtaining Ionic Liquids.*

### *2.1.1. Synthesis of [DBU-PEG][$NTf_2$].*

In a 250 mL round bottom flask, 3.044 g of 1,8-Diazabicyclo[5.4.0]undec-7-ene (DBU), 2.31 g of chloride-polyethylene glycol-chloride ([PEG][Cl]), and acetonitrile solvent were stirred and heated at 80°C for 2 days. It was then roto evaporated at 220 mbar and 50°C until the solvent was fully removed. In a 250 mL round bottom flask, 2.678 g of 8,8′-(3,6-dioxaoctane-1,8-diyl)bis(1,8-diazabicyclo[5.4.0]undec-7-en-8-ium)chloride ([DBU-PEG][Cl]), 2.87 g of lithium bis(trifluoromethanesulfonyl)imide ($LiNTf_2$) and acetonitrile solvent were stirred for 24 hours to perform a cation exchange from chloride to bis(trifluoromethanesulfonyl)imide ($NTf_2$). This was centrifuged at 8000 rpm for 3 minutes to separate the impurities from the ionic liquid, and the ionic liquid was roto evaporated to remove any solvent. Water ($H_2O$) and dichloromethane (DCM) were added to the ionic liquid separate the dissolve and separate the salt from the ionic liquid through density layers. The DCM and ionic liquid mixture was roto evaporated to remove the solvent and isolate the ionic liquid. The sample was then placed in the freeze dryer for 3 hours to separate any excess water out of the ionic liquid. Last, it was placed in the oven for 24 hours, isolating just the ionic liquid, 8,8′-(3,6-dioxaoctane-1,8-diyl)bis(1,8-diazabicyclo[5.4.0]undec-7-en-8-ium)bis(trifluoromethanesulfonyl)imide ([DBU-PEG][$NTf_2$]). The chemical formula for the synthesis of [DBU-PEG][$NTf_2$] is displayed in **Figure 2.1**.

### *2.1.2. [$P_{66614}$][Br].*

The ionic liquid, Trihexyl-tetradecylphosphonium bromide ([$P_{66614}$][Br]), was obtained from Strem Chemicals Inc. **Figure 2.2** shows the chemical structure of [$P_{66614}$][Br].

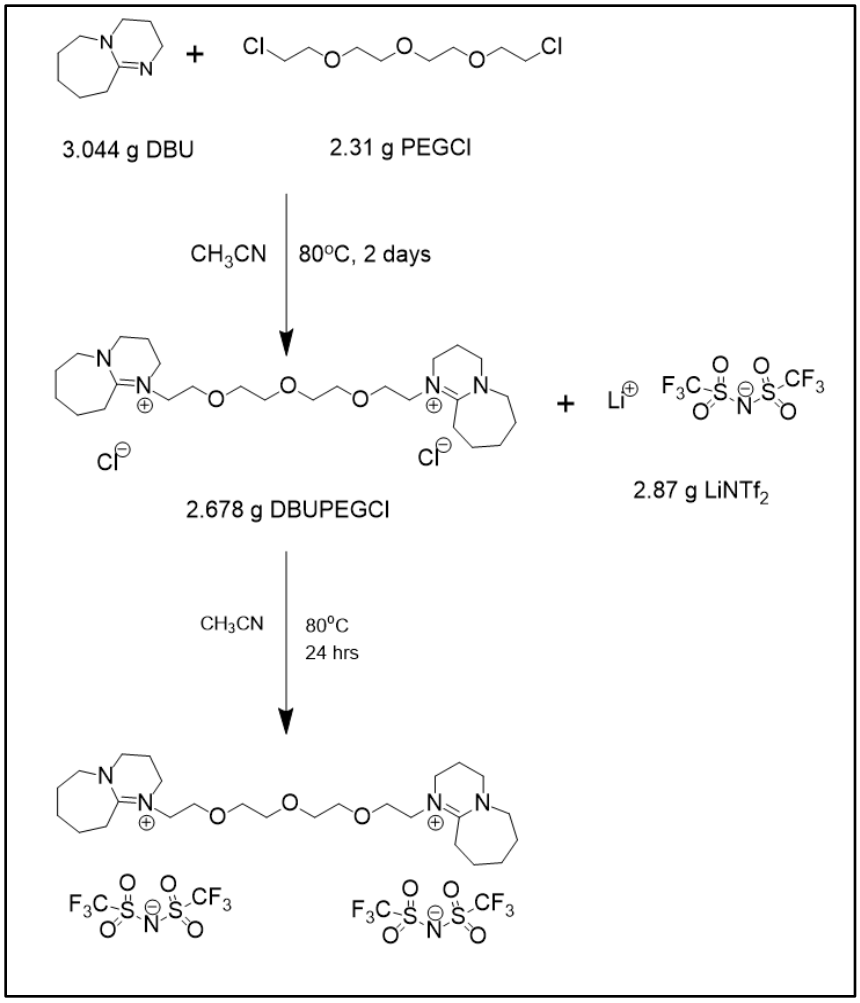


**Figure 2.1. Chemical formula of synthesis of [DBU-PEG][$NTf_2$].**

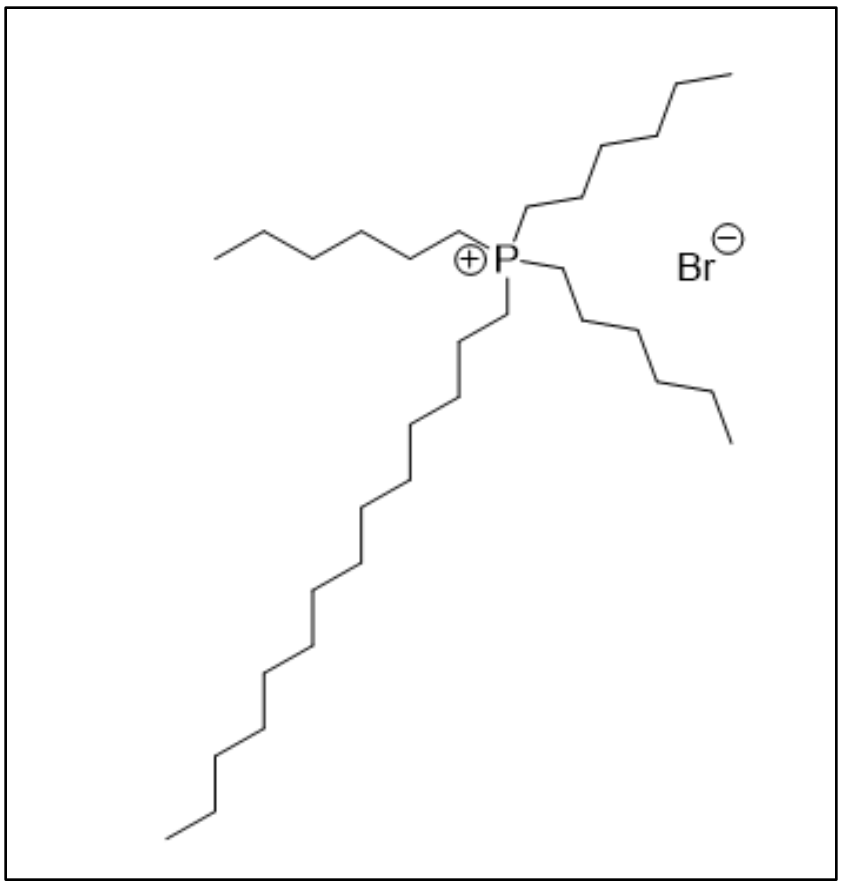


**Figure 2.2. Structure of $[P_{66614}][Br]$.**

### *2.2. Synthesis of zeolites.*

#### *2.2.1. Na-ZSM-5.*

In a large glass vial, 9.6 g of $H_2O$, 6.1 g of Tetrapropylammonium hydroxide (TPAOH), and 6.25 g of tetraethyl orthosillicate (TEOS) were heated and stirred at 80°C for 24 hours. This mixture was then added to a hydrothermal autoclave reactor. A second mixture of 2 g of $H_2O$, 0.23 g of aluminum nitrate, and 0.12 g of sodium hydroxide were stirred until the aluminum nitrate and sodium hydroxide were fully dissolved. This yields a Si/Al ratio of 50/50. The two mixtures were combined in the autoclave reactor, sealed tightly, and placed in the autoclave at 170°C for 24 hours. The sample was washed by water five times by centrifugation at 9000 rpm for 3 minutes to separate out impurities. The zeolite crystal was placed in the freeze dryer for 24 hours to dry out the excess moisture. After, it was placed in the furnace overnight at 550°C with the temperature increasing at a rate of 1 degree/minute for 6 hours. This evaporated the ammonia from the zeolite, leaving only Sodium-Zeolite Socony Mobil-5 (Na-ZSM-5) (**Figure 2.3**).

#### *2.2.2. H-ZSM-5.*

A sample of Na-ZSM-5 was stirred and heated with 2.5 g of ammonium chloride and 50 mL of $H_2O$ at 80°C for 8 hours. This mixture was then washed by water five times at 9000 rpm for 3 minutes. The first two steps of adding ammonium chloride and $H_2O$ and washing by water were repeated two more times to ensure the cation exchange from sodium ($Na^+$) to hydrogen ($H^+$) was fully complete. After the third cation exchange, the zeolite sample was placed in the freeze dryer to dry out the excess moisture. It was placed in the furnace at 550°C with the temperature increasing at a rate of 1 degree/minute for 6 hours to evaporate out the ammonia from the zeolite. This completed the ion exchange from $Na^+$ to $H^+$, leaving just the Hydrogen-Zeolite Socony Mobil-5 (H-ZSM-5) (**Figure 2.4**).

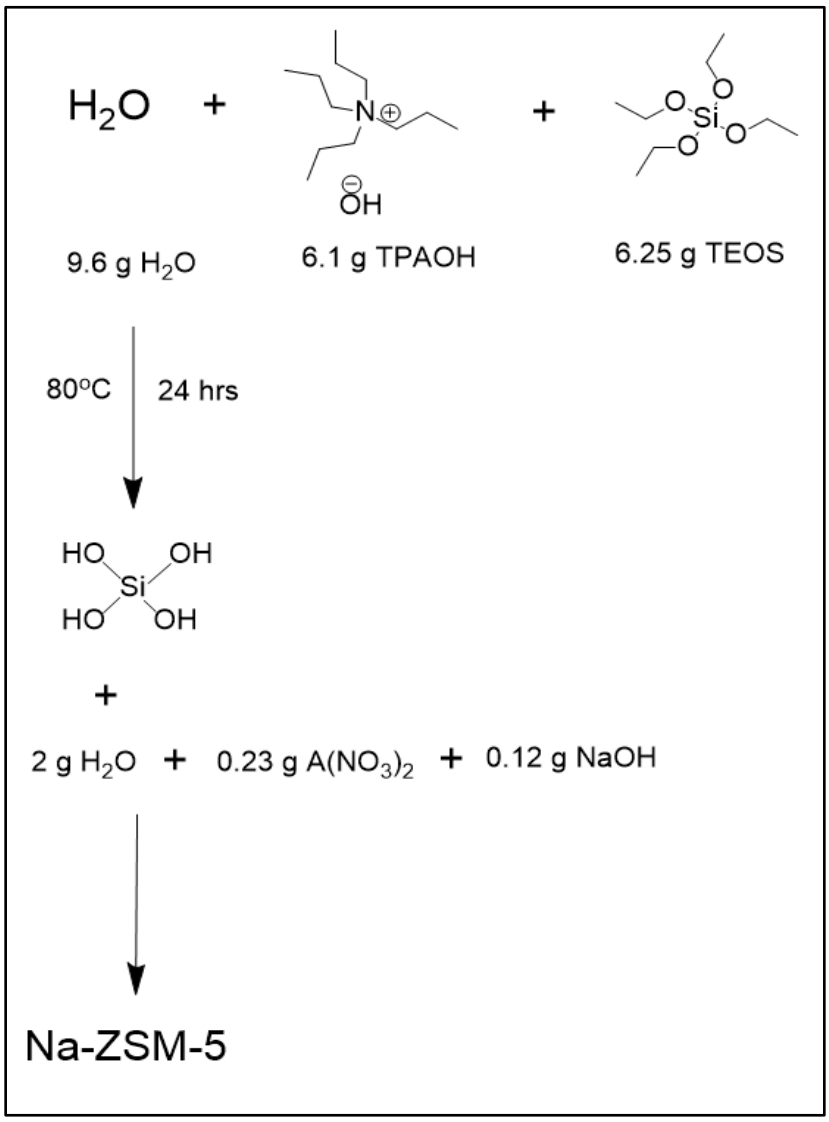


**Figure 2.3. Chemical formula of synthesis of Na-ZSM-5.**

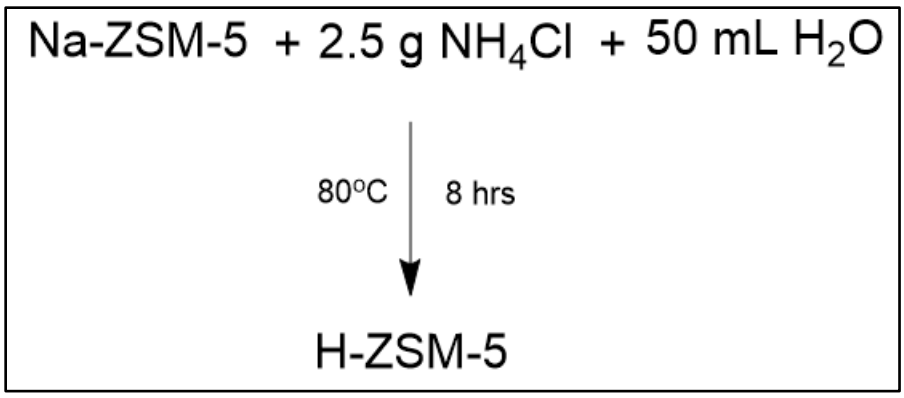


**Figure 2.4. Chemical formula of synthesis of H-ZSM-5.**

### *2.3. Preparation of Porous Liquids.*

Each porous liquid was comprised of a specific weight percent of the zeolite suspended in its paired ionic liquid. Both ionic liquid samples had two porous liquid variations with a porous media weight percent of 10% and 20%. The [DBU-PEG][$NTf_2$] samples were paired with the zeolite, Na-ZSM-5, and the [$P_{66614}$][Br] samples were paired with the zeolite, H-ZSM-5. To prepare the porous liquids, the zeolite component was ultrasonicated with a methanol solvent for one hour to fully dissolve. Then, the ionic liquid was mixed with a methanol solvent and added to the zeolite-methanol mixture. The porous liquid was stirred for 24 hours using a magnetic stir bar to disperse the zeolite evenly throughout the ionic liquid. The sample was heated at 80°C for 2 hours to evaporate out the methanol solvent, isolating the porous liquid sample.

#### *2.3.1. Na-ZSM-5 with [DBU-PEG][ $NTf_2$].*

The 20 weight % (wt%) Na-ZSM-5 with [DBU-PEG][$NTf_2$] porous liquid was prepared with 600 mg of Na-ZSM-5 and 2.4 g of [DBU-PEG][$NTf_2$]. **Figure 2.5** displays the chemical formula of 20 wt% Na-ZSM-5 with [DBU-PEG][$NTf_2$].

The 10 wt% Na-ZSM-5 with [DBU-PEG][$NTf_2$] porous liquid was prepared with 300 mg of Na-ZSM-5 and 2.7 g of [DBU-PEG][$NTf_2$].

#### *2.3.2. H-ZSM-5 with [$P_{66614}$][Br].*

The 20 wt% H-ZSM-5 with [$P_{66614}$][Br] porous liquid was prepared with 600 mg of H-ZSM-5 and 2.4 mg of [$P_{66614}$][Br]. **Figure 2.6** displays the chemical formula of 20 wt% H-ZSM-5 with [$P_{66614}$][Br].

The 10 wt% H-ZSM-5 with [$P_{66614}$][Br] porous liquid was prepared with 300 mg of H-ZSM-5 and 2.7 g of [$P_{66614}$][Br].

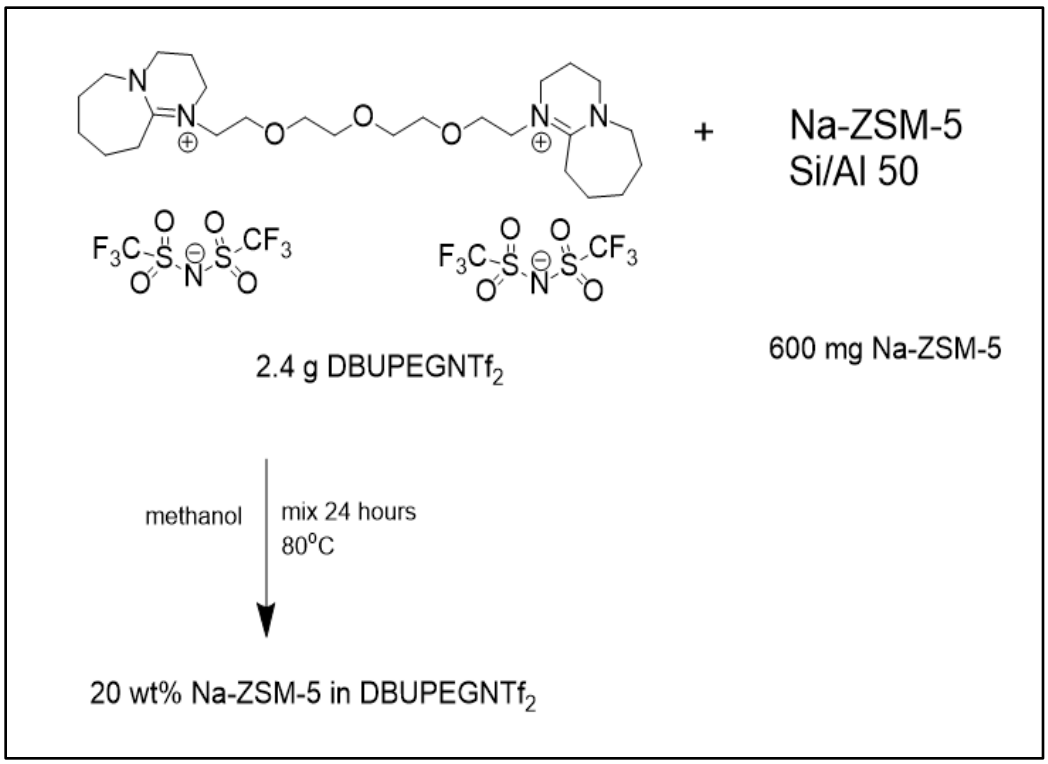


**Figure 2.5. Chemical formula of synthesis of porous liquid 20 wt% Na-ZSM-5 with [DBU-PEG][$NTf_2$].**

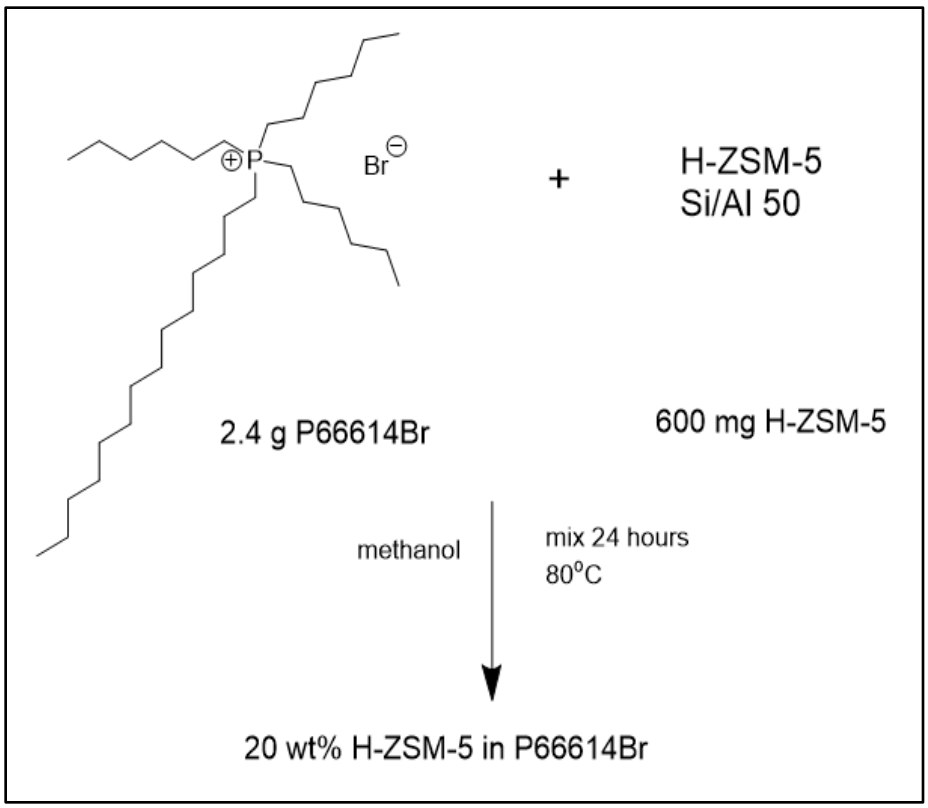


**Figure 2.6. Chemical formula of synthesis of porous liquid 20 wt% H-ZSM-5 with [$P_{66614}$][Br].**

### *2.4. Porous Liquid and Ionic Liquid Characterization.*

#### *2.4.1. BET Isotherm.*

Brunauer-Emmit-Teller (BET) theory explains the adsorption and desorption capabilities of gas molecules on the surface of zeolites. The $N_2$ BET isotherm of Na-ZSM-5 and H-ZSM-5 were obtained using the Micromeritics Gemini VII surface area instrument. Based on the isotherms obtained, the surface area of the zeolites was determined. The surface area was used to describe the accessible surface area that the gas molecules can use for adsorption.

#### *2.4.2. SEM and TEM.*

Scanning electron microscopy (SEM) provides high resolution images of a sample's surface. This was used to measure the size of the zeolite particles, and the images helped when determining which membrane size was the best to load the porous liquids on. Transmission electron microscopy (TEM) provides high resolution images of the internal structure of a sample. This was used to measure the size of the pores in the zeolites. Measuring the pore sizes from TEM ensured the zeolites could capture $CO_2$ molecules in the pores.

#### *2.4.3. NMR and XRD.*

The nuclear magnetic resonance (NMR) spectra was tested to determine the structure of [DBU-PEG][$NTf_2$]. The hydrogen NMR and carbon NMR were compared to a reference NMR of the same ionic liquid to confirm the structure after synthesis. The x-ray diffraction (XRD) spectra of each zeolite was tested to determine their structures. The XRD's obtained were compared to the reference XRD's of the same zeolites to confirm the structures after synthesis.

#### *2.4.4. Viscometer.*

The Brookfield DVII + Pro Viscometer was used to measure the viscosities of the ionic liquids and porous liquids. The 1.0 mL of each sample was used to measure the viscosities at

25°C. This was used to show how adding zeolites to ionic liquids increased the viscosities of the liquids.

### *2.5. Membrane Testing.*

To test the membrane of each porous liquid and ionic liquid, the membrane was soaked in the liquid and placed in a vacuum oven for 24 hours. The vacuum ensures the liquid is evenly dispersed across the membrane. Before placing the membrane in the testing system, the excess liquid was gently brushed off using a kimtech kimwipe. The outer rim of the testing chamber was lightly greased to ensure a tight seal when the chamber is closed. A support membrane with large pores was placed over the bottom chamber to add structural support for the liquid-soaked membrane. The soaked membrane was placed on top of the support membrane and the upper chamber was closed on top. The chamber was sealed tightly, and a vacuum was drawn for 10 hours.

To test the permeability of a gas, the vacuum was closed and the desired gas released into the pressure chamber until the desired pressure was reached. The gas was then released into the membrane and the Logger Pro program started. $[P_{66614}][Br]$ samples were run for an hour gathering 10 data points per minute. [DBU-PEG]$[NTf_2]$ samples were run for three hours gathering 10 data points per minute. Based on the pressure versus time data, the selectivity and permeabilities of $CO_2$ and $N_2$ were determined.

# CHAPTER 3. RESULTS AND DISCUSSION

## *3.1. Characterization of Zeolites, Ionic Liquids, and Porous Liquids.*

### *3.1.1. BET Isotherm and SEM and TEM Images.*

As shown in **Figure 3.1**, The $N_2$ BET isotherms of H-ZSM-5 and Na-ZSM-5 were obtained to measure the adsorption and desorption properties of the zeolite. This gave a surface area accessible for gas adsorption in H-ZSM-5 of 338.6126 $\frac{m^2}{g}$. The surface accessible for gas adsorption in Na-ZSM-5 was 348.0635 $\frac{m^2}{g}$. The isotherms obtained were compared to reference isotherms of H-ZSM-5 and Na-ZSM-5 previously obtained from another project in Dr. Sheng Dai's lab under the same synthesis. The zeolites exhibited a Type 1 isotherm, describing the zeolites as microporous. A Type 1 isotherm is typically observed having an initial rapid adsorption and a plateau where the further adsorption is restricted by the pore size.[8]

To determine the pore size and particle size of the zeolites, SEM and TEM images were obtained. The observed particle size of the ZSM-5 sample was around 200 nm (**Figure 3.2**), and the observed pore size of the ZSM-5 sample was about 0.55nm (**Figure 3.3**). A $CO_2$ gas molecule is about 0.33 nm in diameter, and a $N_2$ gas molecule is 0.346 nm in diameter.[13] Analyzing the pore size of the zeolites ensures the gas molecules can penetrate and adsorb into the zeolite pores. Additionally, knowing the particle size is important when determining what size porous membrane to use. When the porous liquids were soaked into the membranes, the pore size of the membrane needed to be large enough to let the zeolites penetrate in the membrane, but not so large where the porous liquid could be pulled out when the membrane testing chamber is under a vacuumed. Therefore, based on the zeolite particle size of around 200 nm, PES membranes of 450 nm pore size were used.

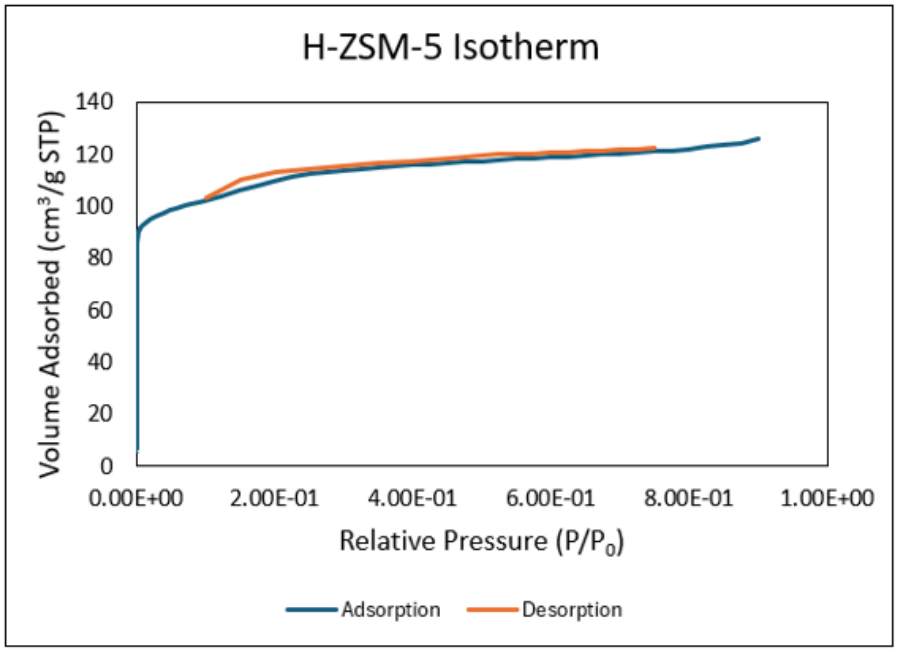


(a)

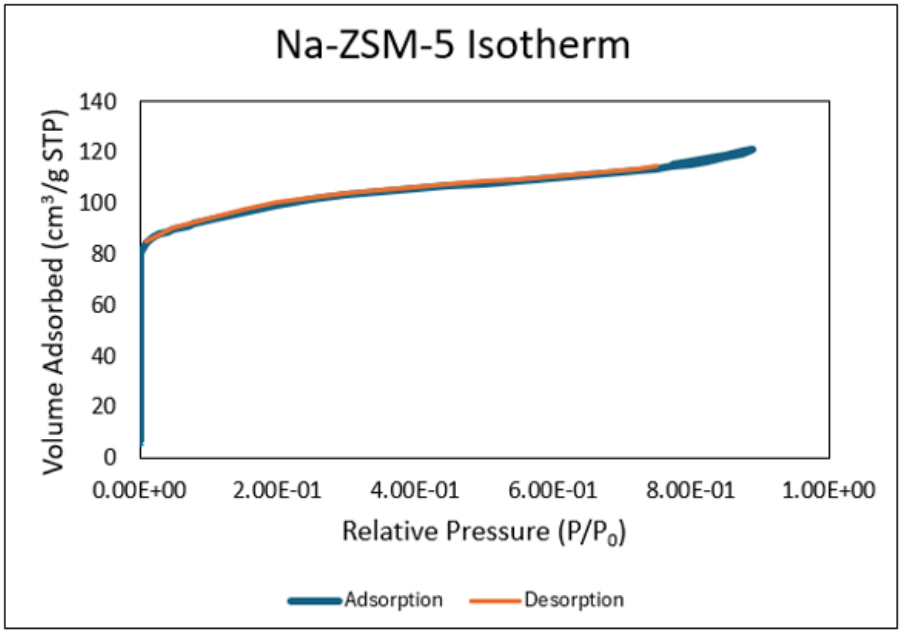


(b)

**Figure 3.1. $N_2$ BET Isotherm of (a) H-ZSM-5 and (b) Na-ZSM-5.**

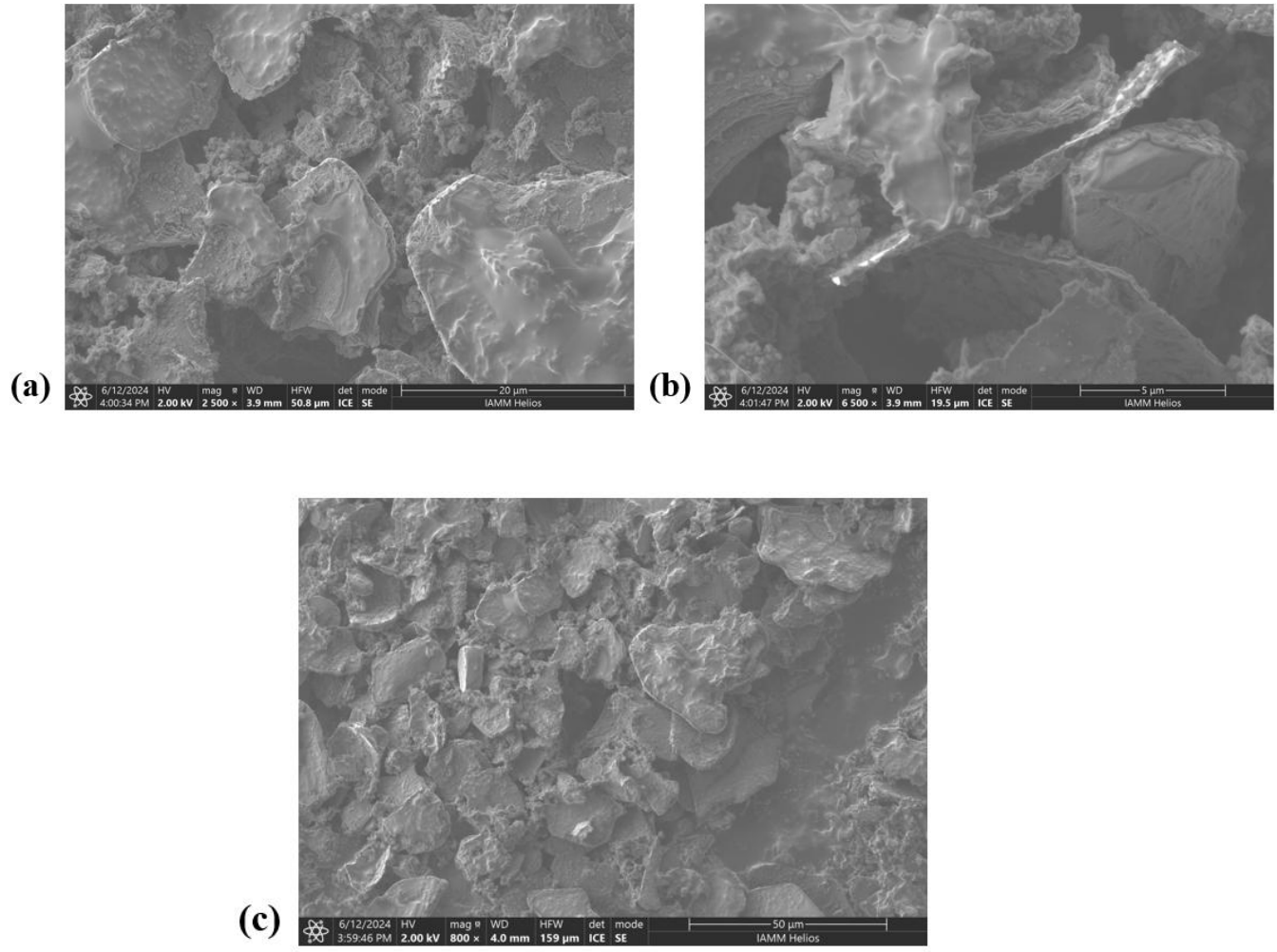


**Figure 3.2. SEM images of the zeolite particles at different magnifications with scale bars of (a) 20 $\mu$m, (b) 5 $\mu$m, and (c) 50 $\mu$m.**

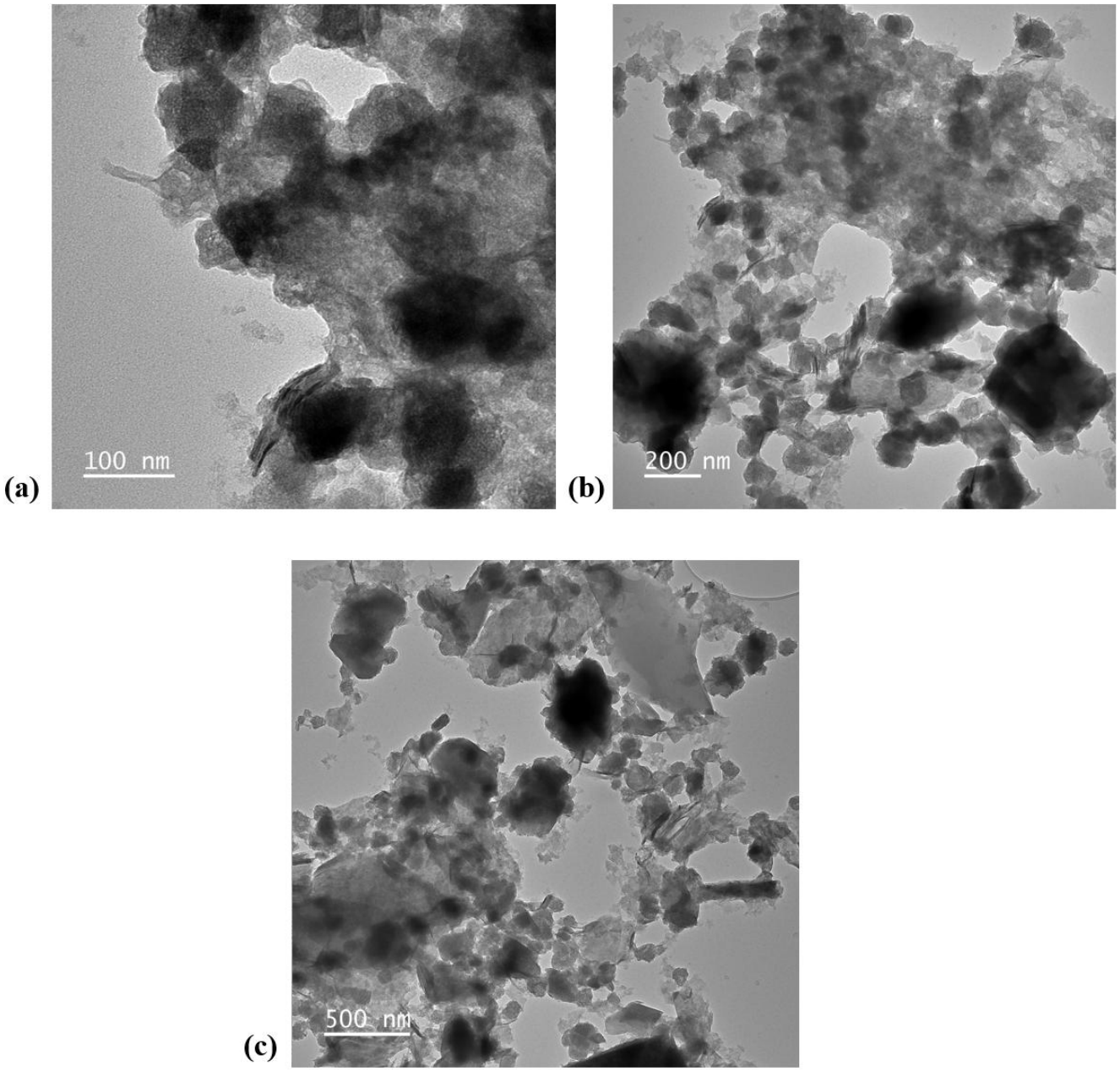


**Figure 3.3. TEM images of the zeolite pores at different magnifications with scale bars of (a) 100 nm, (b) 200 nm, and (c) 500 nm.**

### *3.1.2. XRD and NMR Spectra.*

The XRD spectra of H-ZSM-5 and Na-ZSM-5 were obtained (**Figure 3.4**). Both zeolites had an Al/Si ratio of 50/50. Their spectra were compared to reference XRD's from Krisinandi (2015)[10] and Li (2019)[11] to confirm their structures after synthesis. Both zeolites exhibited strong peaks at 8 and 24 degrees, and weaker peaks at 16, 30, and 47 degrees. The strong peaks at 8 and 24 degrees relates to the pore structure in the Mobil Five (ZSM-5) framework of the zeolite. The peaks in H-ZSM-5 had stronger intensities than those of Na-ZSM-5. In H-ZSM-5, the observed peak at 8 degrees had an intensity of 28086, and the observed peak at 24 degrees had an intensity of 12489. Meanwhile in Na-ZSM-5, the strong peak at 8 degrees had an intensity of 14529, and the peak at 24 degrees had an intensity of 13595. The intensity of the peaks provides some insight into the crystallinity of the samples, as the stronger diffraction peaks suggest a higher degree of crystallinity and improved lattice strain in the H-ZSM-5 sample.

The NMR spectra of [DBU-PEG][$NTf_2$] was obtained to confirm the structure of the ionic liquid after synthesis. The C-NMR and H-NMR were compared to reference NMR's of [DBU-PEG][$NTf_2$] obtained from a previous project in Dr. Sheng Dai's lab under the same synthesis. The ions in [DBU-PEG][$NTf_2$] were identified based on their peaks and multiplets in the C-NMR spectra (**Figure 3.5**). The [DBU] ion was observed as a doublet at 165 ppm, corresponding to the carbon atoms in the imidazolium ring. The [PEG] ion had a strong septet at 40 ppm; triplets at 28, 49, and 54 ppm; doublets at 20, 23, and 25 ppm; and a singlet at 32 ppm. These peaks relate to the repeating ethylene glycol groups in the ion. The anion [$NTf_2$] was observed as a quartet at 120 ppm, corresponding to the interactions between fluorine atoms and carbon atoms. The H-NMR (**Figure 3.6**) observed singlets at 1.5 and 2.8 ppm; a doublet at 2; and a triplet at 3.5 ppm.

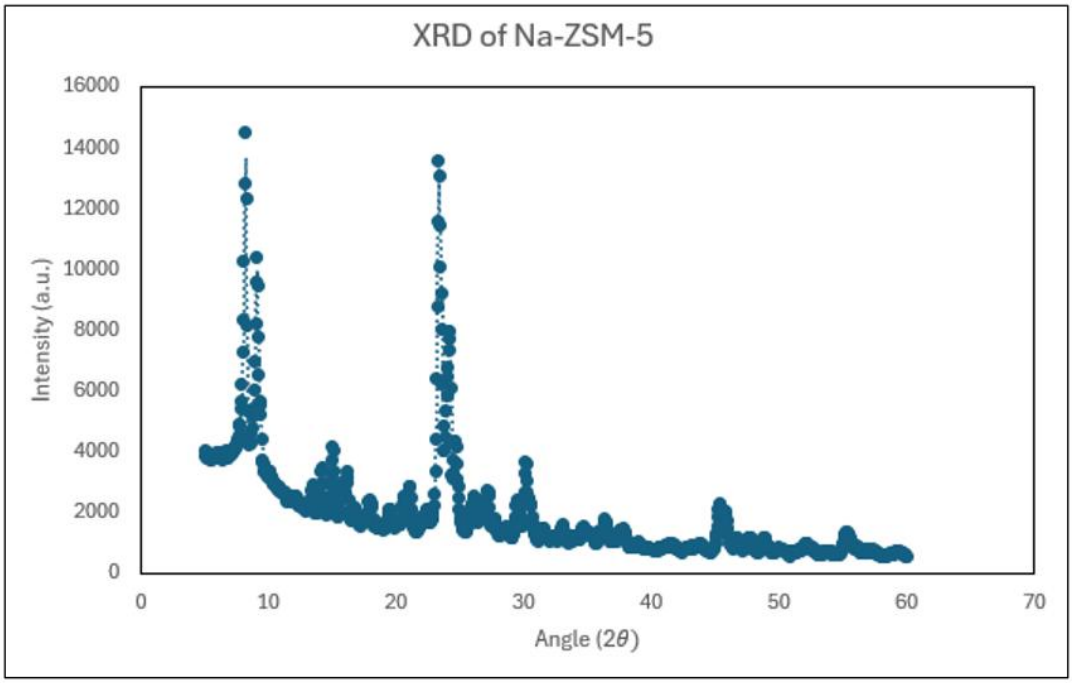


(a)

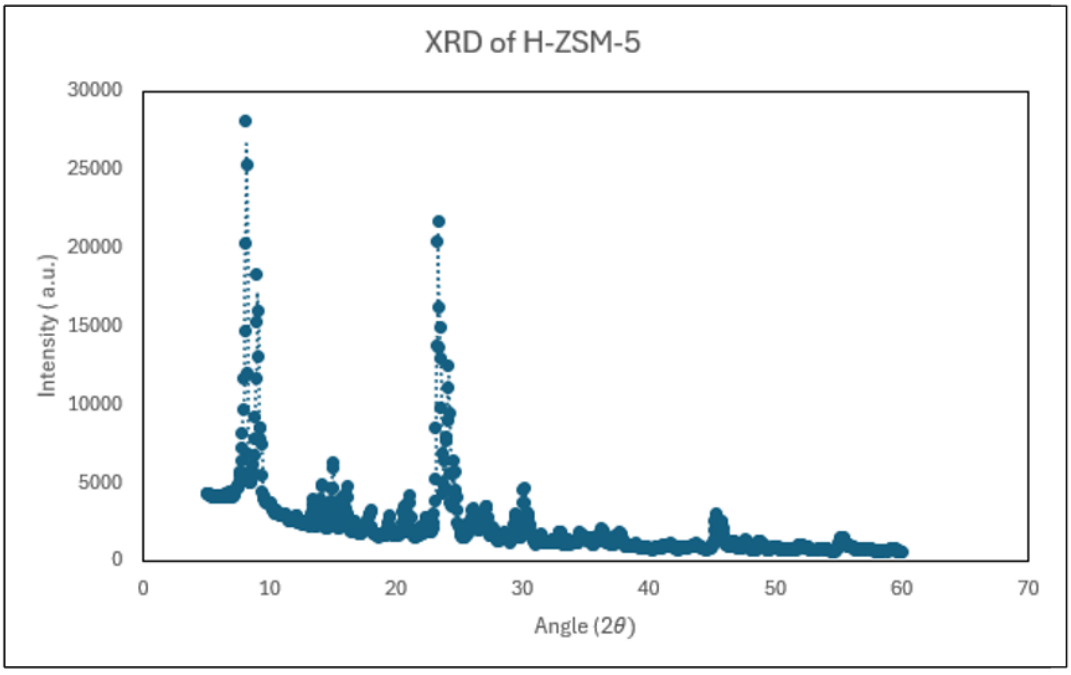


(b)

**Figure 3.4. XRD spectra of (a) Na-ZSM-5 and (b) H-ZSM-5.**

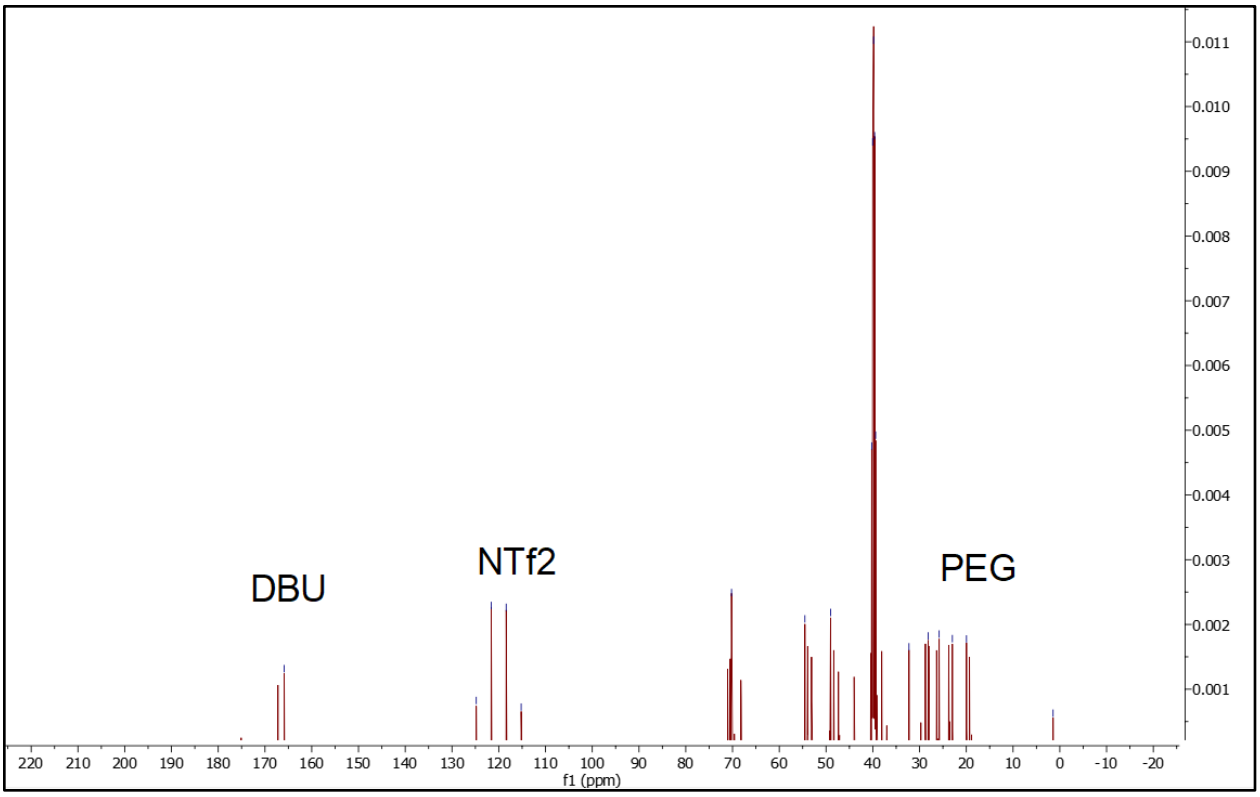


**Figure 3.5. C NMR of [DBU-PEG][$NTf_2$]. (a) [DBU] ion, (b)[$NTf_2$] ion, (c)[PEG] ion.**

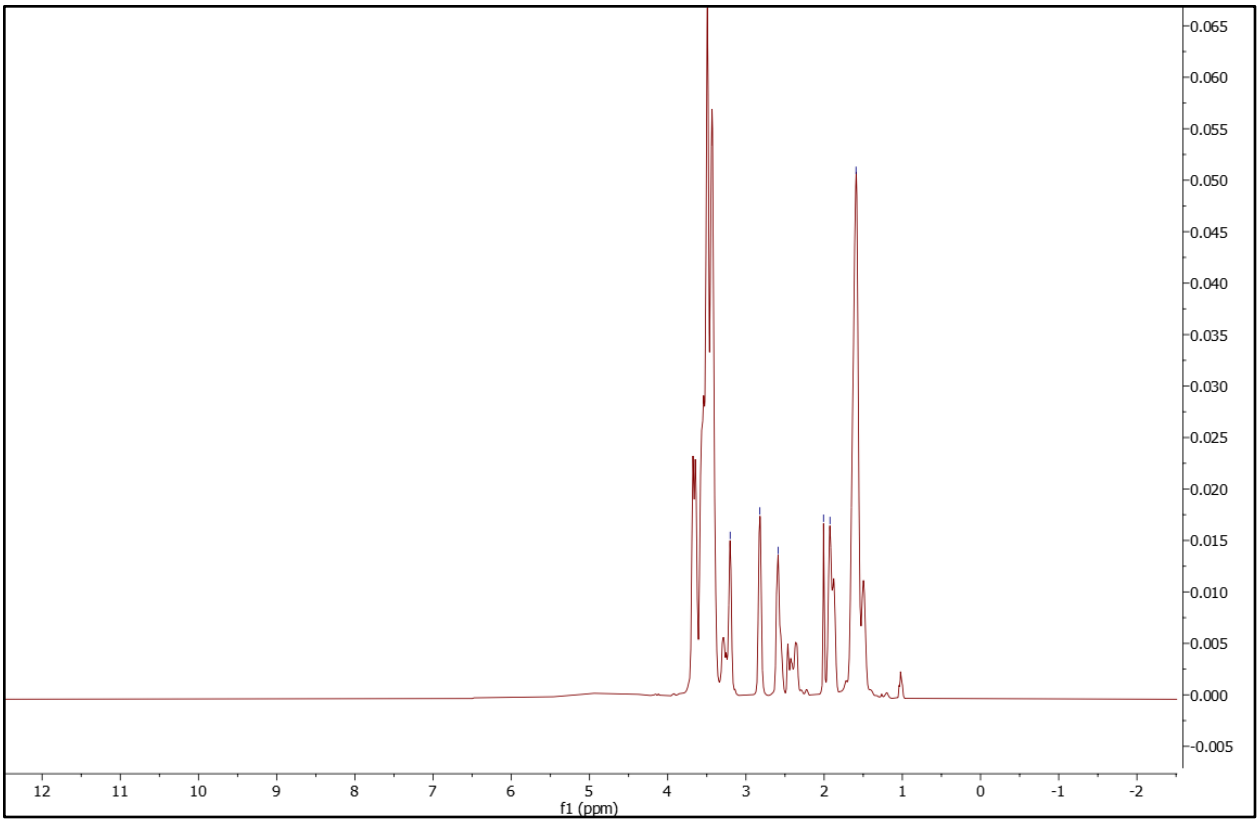


**Figure 3.6. H NMR of [DBU-PEG][$NTf_2$].**

### *3.1.3. Average Viscosities.*

The viscosities of both ionic liquids and all four porous liquids were measured. $[P_{66614}][Br]$ without the zeolite had an average viscosity of 1813.5 cP. When 10 wt% H-ZSM-5 was added, the viscosity increased by a factor of 1.929. This yielded an average viscosity of 3499.0 cP. When 20 wt% H-ZSM-5 was added, the viscosity of the ionic liquid increased by a factor of 3.110 to an average viscosity of 5639.5 cP. As displayed in **Table 3.1**, the overall trend showed the viscosity of the $[P_{66614}][Br]$ increased as the concentration of the zeolites increased.

The average viscosity of [DBU-PEG][$NTf_2$] was observed at 2295.5 cP. The average viscosity increased by a factor of 2.485 when 10 wt% Na-ZSM-5 was added to the ionic liquid. 10 wt% Na-ZSM-5 with [DBU-PEG][$NTf_2$] had an average viscosity of 5704.2 cP. When 20 wt% Na-ZSM-5 was added, the average viscosity of the ionic liquid increased by a factor of 3.901. The average viscosity of 20 wt% Na-ZSM-5 with [DBU-PEG][$NTf_2$] was 8954.9 cP. As displayed in **Table 3.2**, [DBU-PEG][$NTf_2$] also displayed an increasing trend in the average viscosities as the concentration of the zeolites increased.

Comparatively, both ionic liquids had an increase in average viscosities as the zeolite concentrations increased. However, [DBU-PEG][$NTf_2$] had a higher viscosity, and its viscosity increased at a higher rate than $[P_{66614}][Br]$. The viscosity of [DBU-PEG][$NTf_2$] is higher than most ionic liquids, so the mass transfer rate is much slower. This causes limitations when testing the gas separation properties, as slow diffusion requires longer time to separate gases, lowering the efficiency of carbon capture. Having a high viscosity does present some benefit in membrane testing, as it helps the liquid remain in the membrane pores and makes it more resistant to being pulled out of the membrane under varying pressures.

**Table 3.1. Average viscosities of $[P_{66614}][Br]$, 10 wt% H-ZSM-5 with $[P_{66614}][Br]$, and 20 wt% H-ZSM-5 with $[P_{66614}][Br]$.**

| Ionic Liquid/Porous Liquid | Viscosity (cP) |
|---|---|
| $[P_{66614}][Br]$ | 1813.5 cP |
| 10 wt% H-ZSM-5 w $[P_{66614}][Br]$ | 3499.0 cP |
| 20 wt% H-ZSM-5 w $[P_{66614}][Br]$ | 5639.5 cP |

**Table 3.2. Average viscosities of $[DBU\text{-}PEG][NTf_2]$, 10 wt% Na-ZSM-5 with $[DBU\text{-}PEG][NTf_2]$, and 20 wt% Na-ZSM-5 with $[DBU\text{-}PEG][NTf_2]$.**

| Ionic Liquid/Porous Liquid | Viscosity (cP) |
|---|---|
| $[DBU\text{-}PEG][NTf_2]$ | 2295.5 cP |
| 10 wt% Na-ZSM-5 w $[DBU\text{-}PEG][NTf_2]$ | 5704.2 cP |
| 20 wt% Na-ZSM-5 w $[DBU\text{-}PEG][NTf_2]$ | 8954.9 cP |

### *3.2. Membrane testing of [$P_{66614}$][Br], 10 wt% H-ZSM-5 with [$P_{66614}$][Br], and 20 wt% H-ZSM-5 with [$P_{66614}$][Br].*

The membranes of [$P_{66614}$][Br], 10 wt% H-ZSM-5 with [$P_{66614}$][Br], and 20 wt% H-ZSM-5 with [$P_{66614}$][Br] were tested on PES membranes with 450 nm pore size. The gas pressure was kept at 30 kPa while data was collected for 1 hour. **Table 3.3** lists the averages of the gas separation characteristics of all [$P_{66614}$][Br] samples. For [$P_{66614}$][Br], the average $CO_2$ and $N_2$ permeances were 7.045E-10 and 4.883E-11 respectively. The average $\frac{CO_2}{N_2}$ selectivity was 14.449. Finally, the average $CO_2$ permeability was 456.655, and the average $N_2$ permeability was 32.019. When 10 wt% H-ZSM-5 was suspended in [$P_{66614}$][Br], the average $CO_2$ permeance was 1.053E-10, and the average $N_2$ permeance was 7.042E-11. The average $\frac{CO_2}{N_2}$ selectivity increased by a factor of 1.045 to 15.095 in 10 wt% H-ZSM-5 with $\frac{CO_2}{N_2}$ selectivity. The average $CO_2$ and $N_2$ permeabilities also increased to 567.725 and 38.775 respectively. When the porous liquid permeabilities were compared to the permeability values in the ionic liquid, the average $CO_2$ permeability increased by a factor of 1.243 and the average $N_2$ permeability increased by a factor of 1.211. When 20 wt% H-ZSM-5 was suspended in [$P_{66614}$][Br], the average $CO_2$ and $N_2$ permeances increased to 1.029E-09 and 6.769E-11 respectively. The average $\frac{CO_2}{N_2}$ selectivity increased by a factor of 1.058. The average $CO_2$ permeability increased by a factor of 1.390 to 634.650, and the average $N_2$ permeability increased by a factor of 1.304 to 41.760. As the concentration of the zeolites in [$P_{66614}$][Br] increased, the $CO_2$ permeability and $N_2$ permeability increased, and Selectivity increased. Adding zeolites into the ionic liquids adds free volume that allows more $CO_2$ molecules to get trapped in the liquid.

**Table 3.3. Average Gas Separation Characteristics of [$P_{66614}$][Br], 10 wt% H-ZSM-5 with [$P_{66614}$][Br], and 20 wt% H-ZSM-5 with [$P_{66614}$][Br].**

| | $CO_2$ Permeance | $N_2$ Permeance | $\frac{CO_2}{N_2}$ Selectivity | $CO_2$ Permeability | $N_2$ Permeability |
|---|---|---|---|---|---|
| [$P_{66614}$][Br] | 7.045E-10 | 4.883E-11 | 14.449 | 456.655 | 32.019 |
| 10 wt% H-ZSM-5 w [$P_{66614}$][Br] | 1.053E-10 | 7.042E-11 | 15.095 | 567.725 | 38.775 |
| 20 wt% H-ZSM-5 w [$P_{66614}$][Br] | 1.029E-09 | 6.769E-11 | 15.289 | 634.650 | 41.760 |

### *3.3. Membrane Testing of [DBU-PEG][$NTf_2$], 10 wt% Na-ZSM-5 with [DBU-PEG][$NTf_2$], and 20 wt% Na-ZSM-5 with [DBU-PEG][$NTf_2$].*

The membranes of [DBU-PEG][$NTf_2$], 10 wt% Na-ZSM-5 with [DBU-PEG][$NTf_2$], and 20 wt% Na-ZSM-5 with [DBU-PEG][ $NTf_2$] were tested on PES membranes with 450 nm pore size. The gas pressure was kept at 30 kPa while the data was collected for 3 hours. Due to [DBU-PEG][$NTf_2$] having a high viscosity, the $CO_2$ diffusion is slow and requires longer membrane runs than other ionic liquids to gather sufficient data. **Table 3.4** displays the averages of the gas separation characteristics for all the [DBU-PEG][$NTf_2$] samples. The average $CO_2$ and $N_2$ permeances in [DBU-PEG][$NTf_2$] were 2.608E-10 and 7.808E-12 respectively. When 10 wt% Na-ZSM-5 was suspended in [DBU-PEG][$NTf_2$], the $CO_2$ and $N_2$ permeances decreased to 2.270E-10 and 5.107E-12. When the zeolite concentration was increased to 20 wt%, the $CO_2$ and $N_2$ permeances decreased to 1.226E-10 and 2.611E-12. In [DBU-PEG][$NTf_2$], the average $CO_2$ and $N_2$ permeabilities were 214.297 and 6.327 respectively. The average $CO_2$ permeability decreased by a factor of 0.653 to 139.849 when 10 wt% Na-ZSM-5 was added to [DBU-PEG][$NTf_2$]. When 20 wt% Na-ZSM-5 was added, the $CO_2$ permeability decreased by a factor of 0.353 to 75.610. The average $N_2$ permeability decreased by a factor of 0.498 to 3.151 when 10 wt% Na-ZSM-5 was suspended in [DBU-PEG][$NTf_2$]. When 20 wt% Na-ZSM-5 was added, the $N_2$ permeability decreased by a factor of 0.255 to 1.611. The average $\frac{CO_2}{N_2}$ selectivity of [DBU-PEG][$NTf_2$] was 37.093. As the zeolite concentration increased, the selectivity also increased. With 10 wt% Na-ZSM-5, the average $\frac{CO_2}{N_2}$ selectivity increased by a factor of 1.279 to 47.457. When the zeolite concentration increased to 20 wt%, the average $\frac{CO_2}{N_2}$ selectivity increased by a factor of 1.369 to 50.767.

**Table 3.4. Gas Separation Characteristics of [DBU-PEG][$NTf_2$], 10 wt% Na-ZSM-5 with [DBU-PEG][$NTf_2$], and 20 wt% Na-ZSM-5 with [DBU-PEG][$NTf_2$].**

| | $CO_2$ Permeance | $N_2$ Permeance | $\frac{CO_2}{N_2}$ Selectivity | $CO_2$ Permeability | $N_2$ Permeability |
|---|---|---|---|---|---|
| [DBU-PEG][$NTf_2$] | 2.608E-10 | 7.808E-12 | 37.093 | 214.297 | 6.327 |
| 10 wt% Na-ZSM-5 w [DBU-PEG][$NTf_2$] | 2.270E-10 | 5.107E-12 | 47.457 | 139.849 | 3.151 |
| 20 wt% Na-ZSM-5 w [DBU-PEG][$NTf_2$] | 1.226E-10 | 2.611E-12 | 50.767 | 75.610 | 1.611 |

### *3.4. Robeson Plots of [$P_{66614}$][Br] and [DBU-PEG][$NTf_2$] samples.*

The data obtained from the membrane tests of the [$P_{66614}$][Br] and the [DBU-PEG][$NTf_2$] samples were characterized in a Robeson Plot. A Robeson Plot describes the tradeoff between gas selectivity and permeability of a gas. The Robeson Plot upper bound lines represent a gas separation purity of 99%.[5] The equation used to describe the upper bounds of the Robeson Plot is:

$$P_x = k a_{xy}^n$$

Where $P_x$ represents the permeability, k represents the Barrer front factor, $a_{xy}$ represents the selectivity for gases x/y, and n represents the slope. **Table 3.5** describes the $\frac{CO_2}{N_2}$ gas separation parameters used for the 2008 upper bound and the 2015 upper bound.[3] In **Figure 3.7** and **Figure 3.8**, the 2008 upper bound is represented as the red line, and the 2015 upper bound is represented as the black line.

In **Figure 3.7,** the blue triangles represent [$P_{66614}$][Br], the orange circles represent 10 wt% H-ZSM-5 with [$P_{66614}$][Br], and the green squares represent 20 wt% H-ZSM-5 with [$P_{66614}$][Br]. This visual shows an increase in $CO_2$ permeability as the zeolite concentration increases. The plot also displays the slight increase in $\frac{CO_2}{N_2}$ selectivity as the zeolite concentration increases.

In **Figure 3.8,** the blue triangles represent [DBU-PEG][$NTf_2$], the orange circles represent 10 wt% Na-ZSM-5 with [DBU-PEG][$NTf_2$], and the green squares represent 20 wt% Na-ZSM-5 with [DBU-PEG][$NTf_2$]. This visual displays the decrease in $CO_2$ permeability and the increase in $\frac{CO_2}{N_2}$ selectivity as the zeolite concentration increases.

**Table 3.5. Parameters for the 2008 and 2015 Upper Bounds to describe $\frac{CO_2}{N_2}$ gas separation.**

| | k (Barrer) | n (Slope) |
|---|---|---|
| 2008 Upper Bound | $30.967 \times 10^6$ | $-2.888$ |
| 2015 Upper Bound | $755.58 \times 10^6$ | $-3.409$ |

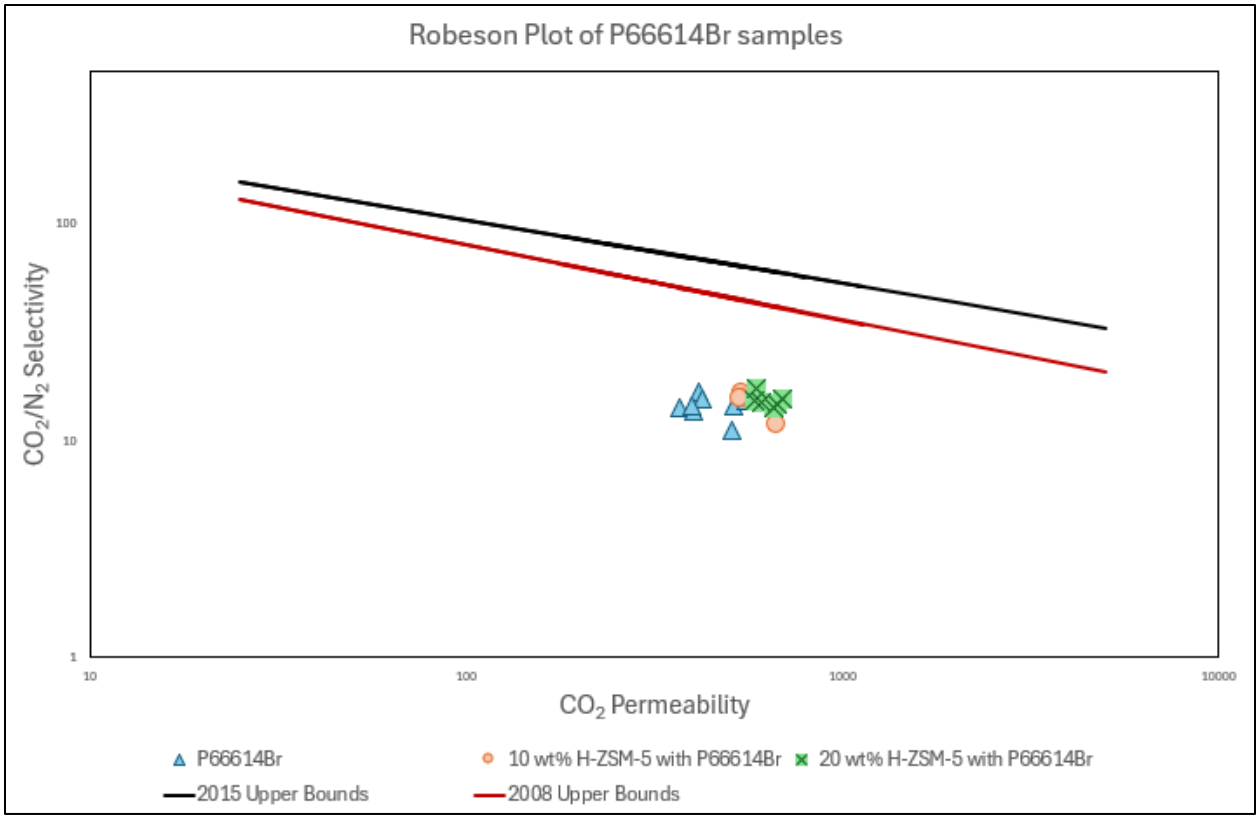


**Figure 3.7. Robeson Plot of $[P_{66614}][Br]$, 10 wt% H-ZSM-5 with $[P_{66614}][Br]$, and 20 wt% H-ZSM-5 with $[P_{66614}][Br]$.**

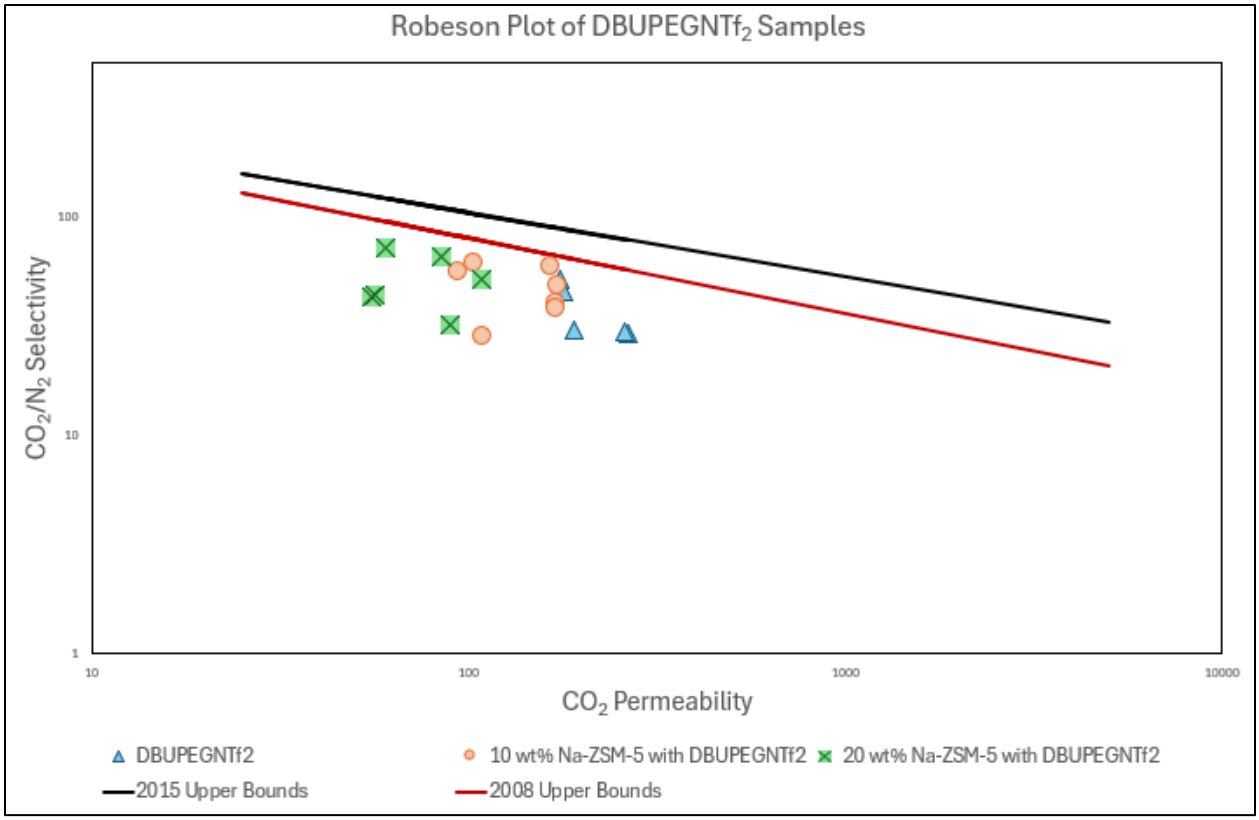


**Figure 3.8. Robeson Plot of [DBU-PEG][$NTf_2$], 10 wt% Na-ZSM-5 with [DBU-PEG][$NTf_2$], and 20 wt% Na-ZSM-5 with [DBU-PEG][$NTf_2$].**

# CHAPTER 4. CONCLUSION

This study provided valuable insight into the gas separation characteristics of ionic liquids and porous liquids, with an emphasis on understanding gas separation behavior and the role zeolites play in modifying these properties. The addition of zeolites into ionic liquids showed an influence in the gas separation properties by changing the $\frac{CO_2}{N_2}$ selectivity and $CO_2$ and $N_2$ permeabilities. Specifically, the addition of H-ZSM-5 into $[P_{66614}][Br]$ increased the $\frac{CO_2}{N_2}$ selectivity and increased the $CO_2$ and $N_2$ permeabilities. Additionally, as the concentration of zeolites increased, there was a greater increase in the selectivity and permeability values. In contrast, when Na-ZSM-5 was added to [DBU-PEG][$NTf_2$], there was an increase in the $\frac{CO_2}{N_2}$ selectivity, but the $CO_2$ and $N_2$ permeabilities both decreased. As the zeolite concentration increased, the $\frac{CO_2}{N_2}$ selectivity had a larger increase, while the permeabilities of $CO_2$ and $N_2$ had more of a decrease.

These trends suggest that incorporating zeolites into ionic liquids offers a promising approach for optimizing gas separation characteristics. The ability to adjust gas separation properties by altering the zeolite and ionic liquid pairs and the concentration of zeolites could have significant implications for industrial applications. Further research is needed to fully understand how adding free volume influences mass transfer mechanisms. Future characterization methods could include FT-IR and Mass-Spectrometry to understand the mass transfer processes and the adsorption of $CO_2$ at different pressures over time. Additionally, investigating other zeolite-ionic liquid pairs would give further insights into these findings and a greater potential for enhancing gas separation. While the results suggest that incorporating

zeolites into ionic liquids can influence gas separation, there is still much to explore to better comprehend the role zeolites and porous liquids play in gas separation.

## REFERENCES


1) Ahmad, M. Z.; Fuoco, A. Porous Liquids – Future for $CO_2$ Capture and Separation? Current Research in Green and Sustainable Chemistry 2021, 4, 100070.
2) An, X.; Wang, P.; Ma, X.; Du, X.; Hao, X.; Yang, Z.; Guan, G. Application of Ionic Liquids in $CO_2$ Capture and Electrochemical Reduction: A Review. Carbon Resources Conversion 2023, 6 (2), 85–97.
3) Bibiana Comesaña-Gándara; Chen, J.; C. Grazia Bezzu; Carta, M.; Rose, I.; Ferrari, M.-C.; Esposito, E.; Fuoco, A.; Jansen, J. C.; McKeown, N. B. Redefining the Robeson Upper Bounds for $CO_2/CH_4$ and $CO_2/N_2$ Separations Using a Series of Ultrapermeable Benzotriptycene-Based Polymers of Intrinsic Microporosity. Energy and Environmental Science 2019, 12 (9), 2733–2740.
4) Boer, D. G.; Langerak, J.; Pescarmona, P. P. Zeolites as Selective Adsorbents for $CO_2$ Separation. ACS Applied Energy Materials 2023, 6 (5), 2634–2656.
5) Castro-Dominguez, B.; Leelachaikul, P.; Messaoud, S. B.; Takagaki, A.; Sugawara, T.; Kikuchi, R.; Oyama, S. T. The Optimal Point within the Robeson Upper Boundary. Chemical Engineering Research and Design 2015, 97, 109–119.
6) Fulvio, P. F.; Dai, S. Porous Liquids: The next Frontier. *Chem* 2020, *6* (12), 3263–3287.
7) Gunawardene, O. H. P.; Gunathilake, C. A.; Vikrant, K.; Amaraweera, S. M. Carbon Dioxide Capture through Physical and Chemical Adsorption Using Porous Carbon Materials: A Review. Atmosphere 2022, 13 (3), 397.
8) Kolesnikov, A.; Budkov, Y. A.; Gor, G. Models of Adsorption-Induced Deformation: Ordered Materials and Beyond. Journal of Physics Condensed Matter 2021, 34 (6), 063002–063002.

9) Kosinov, N.; Gascon, J.; Kapteijn, F.; Hensen, E. J. M. Recent Developments in Zeolite Membranes for Gas Separation. Journal of Membrane Science 2016, 499, 65–79.

10) Krisnandi, Y. K.; Samodro, B. A.; Sihombing, R.; Howe, R. F. Direct Synthesis of Methanol by Partial Oxidation of Methane with Oxygen over Cobalt Modified Mesoporous H-ZSM-5 Catalyst. Indonesian Journal of Chemistry 2015, 15 (3), 263–268.

11) Li, P.; Chen, H.; Schott, J. A.; Li, B.; Zheng, Y.; Mahurin, S. M.; Jiang, D.; Cui, G.; Hu, X.; Wang, Y.; Li, L.; Dai, S. Porous Liquid Zeolites: Hydrogen Bonding-Stabilized H-ZSM-5 in Branched Ionic Liquids. Nanoscale 2019, 11 (4), 1515–1519.

12) Lindsey, R. Climate Change: Atmospheric Carbon Dioxide. Climate.gov.

13) Mehio, N.; Dai, S.; Jiang, D. Quantum Mechanical Basis for Kinetic Diameters of Small Gaseous Molecules. The Journal of Physical Chemistry A 2014, 118 (6), 1150–1154.

14) NASA. World of Change: Global Temperatures. Earth Observatory.

15) O'Reilly, N., Giri, N. and James, S. (2007), Porous Liquids. Chemistry – A European Journal, 13: 3020-3025.

16) Riebeek, H. The Carbon Cycle. NASA.

17) Shan, W.; Fulvio, P. F.; Kong, L.; Schott, J. A.; Do-Thanh, C.-L.; Tian, T.; Hu, X.; Mahurin, S. M.; Xing, H.; Dai, S. New Class of Type III Porous Liquids: A Promising Platform for Rational Adjustment of Gas Sorption Behavior. ACS Applied Materials & Interfaces 2017, 10 (1), 32–36.

18) Supasitmongkol, S.; Styring, P. High $CO_2$ Solubility in Ionic Liquids and a Tetraalkylammonium-Based Poly(Ionic Liquid). Energy & Environmental Science 2010, 3 (12), 1961.

19) United States Environmental Protection Agency. Inventory of U.S. Greenhouse Gas Emissions and Sinks. US EPA.

20) ZSM-5. Famousmaterials.com.

# VITA

Kristina Armstrong was born in Atlanta, Georgia, and raised in Lilburn, Georgia. She pursued her undergraduate degree at Columbus State University, where she studied chemistry with a concentration in biochemistry. During her time at Columbus State University, she was a successful student athlete on the Track and Field team, was involved in numerous organizations, and participated in undergraduate research under Dr. Anil Banerjee. She completed her Bachelor of Arts in Chemistry in May 2023. Kristina later moved to Knoxville, Tennessee to pursue her master's degree at the University of Tennessee-Knoxville. Here, she studied Environmental Chemistry and worked as a teaching assistant and tutor for general chemistry classes. She participated in graduate research under Dr. Sheng Dai at the University of Tennessee and Oak Ridge National Lab, where she researched using ionic liquids and porous liquids for carbon capture. Kristina is anticipated to graduate with her master's degree in August 2025.